Journal of Solid State Chemistry 262 (2018) 8–15

Contents lists available at ScienceDirect

Journal of Solid State Chemistry

journal homepage: www.elsevier.com/locate/jssc

B-site cation order/disorder and their valence states in $Ba_3MnNb_2O_9$ perovskite oxide

Yan Xin[a,*], Qing Huang[b], Zahra Shafieizadeh[c], Haidong Zhou[b]

[a] National High Magnetic Field Laboratory, Florida State University, Tallahassee, FL 32310, USA
[b] Department of Physics and Astronomy, University of Tennessee, Knoxville, TN 37996, USA
[c] Department of Physics, Florida State University, Tallahassee, FL 32306, USA

ARTICLE INFO

Keywords:
EELS
Transition metal valence
Perovskite oxides
B-site ordering
STEM

ABSTRACT

Polycrystalline samples $Ba_3MnNb_2O_9$ synthesized by solid state reaction and single crystal samples grown by optical floating zone have been characterized using scanning transmission electron microscopy and electron energy loss spectroscopy. Three types of B-site Mn and Nb ordering phase are observed: fully ordered 1Mn:2Nb; fully disordered; nano-sized 1Mn:1Nb ordered. No electronic structure change for crystals with different ordering/disordering. The Mn valence is determined to be 2+, and Nb valence is 5+. Oxygen 2p orbitals hybridize with Mn 3d and Nb 4d orbitals. Factors that affect the electron energy loss near edge structures of transition metal white-lines in electron energy loss spectroscopy are explicitly illustrated and discussed.

1. Introduction

Perovskite-related transition metal oxides are among the most intriguing material systems in the field of solid state chemistry and physics. Their physical properties are significantly affected by the changes in chemistry and crystal structure, which is brought about by B-site cation ordering or disordering. Perovskite $Ba(B'_{1/3}B''_{2/3})O_3$ (B = Mn, Ni or Co) is a family of important ceramic materials with desirable dielectric properties suitable for microwave wireless communication applications. In particular, ordered $Ba(B'_{1/3}B''_{2/3})O_3$ or the triple perovskite $Ba_3BNb_2O_9$ has shown multiferroicity [1,2], as photocatalyst [3], and improved microwave dielectric properties [4]. These perovskites can be synthesized by hydrothermal [5], solid state reaction [1,6], aqueous solution [6] and optical floating zone methods. The cation ordering of these perovskites affects their dielectric properties and magnetic ground states. It has been shown that dielectric properties strongly depend on B-site ordering [7]. Using conventional high resolution transmission electron microscopy (HRTEM) imaging and neutron scattering, Liu et al. [6] found that $Ba_3MnNb_2O_9$ samples obtained by solid state reaction are predominately ordered phase; in contrast, samples obtained by aqueous solution are an exclusively disordered phase.

$Ba_3MnNb_2O_9$ is one of the magnetically and geometrically frustrated materials, which has attracted intense research interests in recent years since the inherent spin structure of these materials exhibits new and unusual magnetic phases. The ordered $Ba_3MnNb_2O_9$, for example, is one of a few existing spin 5/2 triangular antiferromagnetic materials. Its negative Curie-Weiss constant suggests a magnetic transition from paramagnetic to antiferromagnetic ordering at 3.5 K [1]. In fact, its two-dimensional triangular lattice with antiferromagnet ordering even shows short-range antiferromagnetic interaction above its Néel temperature T_N [8].

Accurate knowledge of the microstructures and atomic ordering of this material lead to clear understanding of its physical properties, such as its magnetic properties or magnetic ground state. In this paper, we use atomic resolution high-angle-annular-dark-field scanning transmission electron microscopy (HAADF-STEM) imaging techniques to study the order/disorder of Mn and Nb in $Ba_3MnNb_2O_9$ grown by optical floating-zone, also by solid state reaction methods, and use electron-energy-loss spectroscopy (EELS) core-loss spectrum to investigate the electronic structure and B-site cation valence.

2. Experimental

Two types of samples are studied in this paper. One is polycrystalline samples synthesized by solid state reaction, and the other is single crystal samples grown by optical floating zone (OFZ) method.

For polycrystalline samples, stoichiometric mixtures of $BaCO_3$, Nb_2O_5, and MnO powders were ground together, and pressed into pellets and calcined in air at 1230 °C for 24 h. Single crystal was grown by an optical floating zone furnace, which is equipped with two halogen lamps and double ellipsoidal mirrors. In order to prepare for the single

---

[*] Corresponding author.
E-mail address: xin@magnet.fsu.edu (Y. Xin).

https://doi.org/10.1016/j.jssc.2018.02.013
Received 5 January 2018; Received in revised form 14 February 2018; Accepted 15 February 2018

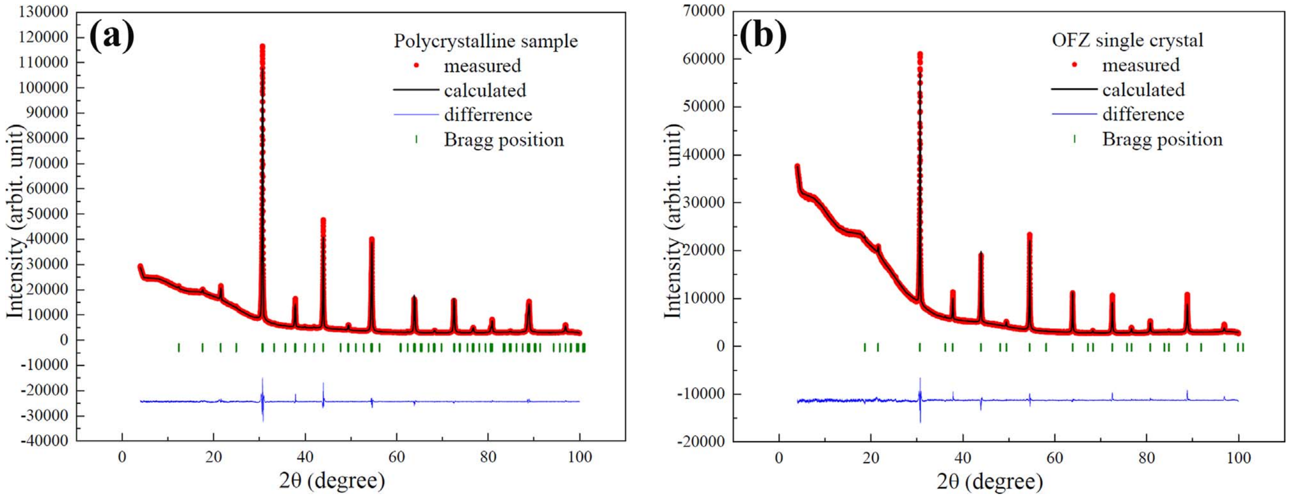

Fig. 1. X-ray diffraction pattern acquired at room temperature from powdered (a) polycrystalline sample; (b) OFZ single crystal.

crystal growth, the polycrystalline sample powder was pressed under 400 atm hydrostatic pressure into feed and seed rods, which were 6 mm in diameter, 60 mm long, and was calcined in Ar gas at 1230 °C for 12 h. The crystal growth, which was controlled at a rate of 10 mm/hour, was carried out in argon gas with feed and seed rods rotating in opposite directions at 25 rpm during growth.

Powder X-ray diffraction data were collected on both powdered polycrystalline and OFZ single crystal samples at room temperature using Cu Kα1 radiation ($\lambda = 1.54051$ Å). The data were analyzed using the Rietveld refinement method. Magnetic susceptibility of the OFZ single crystal sample was measured as a function of temperature using a SQUID magnetometer. For SQUID measurements, the sample was cooled in zero field to 2 K; then the susceptibility data was taken while warming the sample to 300 K in a 1 T magnetic field.

TEM samples were prepared by crushing samples in ethanol with a mortar and pestle. Subsequently, this ethanol suspension of crushed crystals was dropped with a pipette onto a 200 µm mesh TEM copper grid which is coated with a holey carbon film.

STEM study was carried out on a probe-aberration-corrected, cold-field-emission JEM JEOL-ARM200cF at 200 kV, equipped with a Gatan Orius camera, a JEOL HAADF-STEM detector and a Gatan GIF Quantam963 with DualEELS capability. The STEM resolution is 0.078 nm, and energy resolution is 0.5 eV at full emission.

HAADF-STEM images were acquired using a spot size 7c, 30 µm condense lens aperture, at an image scan speed of 32 μs/pixel. The beam convergent angle was 21 mrad, and the STEM image collection angle was from 68 mrad to 174 mrad. Core-loss EELS spectra for Mn, Nb, and O were collected to investigate the valence and electronic structure of samples with different B-site ordering. They were collected in TEM diffraction mode at 8 cm camera length with a 2.5 mm slit at an energy dispersion of 0.1 eV. The electron beam was focused into a crystal area of about 80–100 nm in diameter. The convergence angle is 7.6 mrad and EELS collection angle 17.4 mrad. Each core-loss spectrum was acquired in 2 s using DualEELS, which enables zero loss peak (ZLP) to be simultaneously collected with core-loss spectrum.

Several crystal pieces were studied for each different phase. For each crystal piece with size of roughly 1–2 µm, about 9 spectra were collected. Although we found no difference in energy-loss-near-edge structure (ELNES) between spectra taken from different crystal orientations, all core-loss spectra were taken along the same crystal orientation for easy comparison. Before we started acquiring each individual EELS spectrum, we first deleted the spectrometer dark current background file so that a new dark current background would be automatically acquired for each spectrum, thus avoiding a fixed noise pattern. We examined the sample area after each individual spectrum was taken to ensure that the EELS data were collected on pristine crystal without any beam damage.

3. Results and discussion

3.1. X-ray diffraction and magnetic property

The Rietveld refinement of room temperature X-ray diffraction from powdered crystals (Fig. 1a and b) has identified two crystal phases. The polycrystalline sample has an ordered B-sites phase (Table 1). For the ordered phase, the standard formula is $Ba_3MnNb_2O_9$, where the Mn and Nb sites have the ordering of 1Mn:2 Nb (–Mn-Nb-Nb-Mn-Nb-Nb-….). This material is a triple perovskite, has a P-3m1 trigonal structure, and lattice parameters of a = 0.5816 nm and b = 0.7146 nm, in agreement with what was reported before [1,9].

For the OFZ single-crystal sample, the best refinement model is $Ba_2(Mn_{2/3}Nb_{1/3})NbO_6$, which has a cubic structure with Fm-3m symmetry and a lattice parameter of 0.8235 nm (Table 2). This structure is not completely randomly disordered with 1/3Mn : 2/3Nb on all the B-sites, since some B-site has mixed Mn and Nb, and some sites just have Nb. However, the calculated pattern from this model shows two peaks at 18° and 36°, which are missing from the experimental pattern. But for a completely disordered B-site phase, $Ba(Mn_{1/3}Nb_{2/3})O_3$ that has a higher symmetry, leads to the absence of these two Bragg peaks. This uncertainty by X-ray diffraction modeling is related to the TEM observation shown below as the OFZ single crystal has a disordered matrix with nano-sized ordered phases.

The temperature dependence of molar magnetic susceptibility of

Table 1
Refined structural parameters of polycrystalline sample.

Polycrystal sample a = b = 5.81563(4) Å, c = 7.14604 (6) Å, overall B factor = 0.13405 Å^2 Space group: P-3m1

Atom	Site	X	Y	Z	Occ.
Ba1	2d	0.3333	0.6667	0.6656	0.16667
Ba2	1a	0	0	0	0.08333
Mn	1b	0	0	0.5	0.08333
Nb	2d	0.3333	0.6667	0.1671(4)	0.16667
O1	3e	0.5	0	0	0.25
O2	6i	0.1859(7)	0.3717(14)	0.2726(4)	0.5
Bond distance(Å)					
Nb-O1	2.060(1)				
Nb-O2	1.666(3)				
Mn-O2	2.479(3)				